MODELING COLLOID TRANSPORT IN SATURATED POROUS MEDIA: AN ASSESSMENT OF THE IMPORTANCE OF pH AND KINETICS IN VIRUS TRANSPORT

by

Stephen Hinkle

A Thesis Submitted to the Faculty of the

DEPARTMENT OF HYDROLOGY AND WATER RESOURCES

In Partial fulfillment of the Requirements
For the Degree of

MASTER OF SCIENCE
WITH A MAJOR IN HYDROLOGY

In the Graduate College

THE UNIVERSITY OF ARIZONA

1990

STATEMENT BY AUTHOR

This thesis has been submitted in partial fulfillment of requirements for an advanced degree at The University of Arizona and is deposited in the Universtiy Library to be made available to borrowers under rules of the Library.

Brief quotations from this thesis are allowable without special permission, provided that accurate acknowledgement of source is made. Requests for permission for extended quotation from or reproduction of this manuscript in whole or in part may be granted by the head of the major department of the Dean of the Graduate College when in his or her judgement the proposed use of the material is in the interests of scholarship. In all other instances, however, permission must be obtained from the author.

SIGNED Stephen Hale

APPROVAL BY THESIS CO-DIRECTORS

This thesis has been approved on the date shown below:

R. C. Bales
Professor of Hydrology

March 8, 1990
Date

C. P. Gerba
Professor of Microbiology

March 8, 1990
Date

ACKNOWLEDGEMENTS

I would like to thank my advisors, Dr. Roger C. Bales and Dr. Charles P. Gerba, of the University of Arizona's Departments of Hydrology and Water Resources and of Microbiology and Immunology, respectively, for their guidance, clear instruction, and encouragement throughout the course of this research. I would also like to thank Nancy Ward of the Department of Hydrology and Water Resources, University of Arizona, for conducting the N_2 adsorption analyses. Finally, I would like to thank my wife, Mary Lynn Scattaregia, for her patience and understanding during the long nights I spent in the laboratory.

TABLE OF CONTENTS

LIST OF FIGURES

LIST OF TABLES

ABSTRACT

Virus sorption and transport were investigated in controlled laboratory column experiments. Bacteriophage PRD1 did not sorb to silica beads at pH 7 but sorbed strongly at pH 5.5. Kinetic nonequilibrium prevailed at pH 5.5. Desorption of phage was detected during 27 pore volumes of desorption under steady-state conditions and during 135 pore volumes of desorption under transient conditions. Long tailing in the desorption limbs of the breakthrough curves suggests slow desorption rates. Advection-dispersion modeling of the experimental results with a pseudo-first-order reversible-sorption model provided a means by which to estimate transport parameters. Modeling results suggest that the pseudo-first-order rate coefficient for desorption of PRD1 from silica beads at pH 5.5 lies between 2.5×10^{-7} s^{-1} and 6.7×10^{-6} s^{-1}. Desorption was strongly pH dependent, and sorbed phage were eluted by raising solution pH. Column effluent concentrations of over fourteen times original input concentrations were measured during desorption at elevated pH, suggesting that significant chemical perturbations can in some instances contribute more to colloid desorption than desorption rates applied over long periods of time in steady-state systems.

INTRODUCTION

Colloids are an integral part of the aquatic environment. Colloids are particles less than ten microns in diameter [*Stumm and Morgan, 1981*]; as such, water-borne colloids are subject to negligible gravitational settling. Colloids include biologically active or potentially active particles, inactive organic particles, and inorganic particles. Inorganic colloids include mineral fragments, clay minerals, and amorphous compounds. Inorganic colloids often contain coatings of organic matter.

Colloidal surfaces generally carry an electrostatic charge. Three mechanisms are thought to be responsible for creating charged surfaces on colloidal particles. Amphoteric functional groups ionize to impart an electrostatic charge to a surface; most metal oxides and viruses exhibit amphoteric behavior. Lattice imperfections and isomorphic substitution in clay minerals result in charged surfaces. Finally, a surface charge may result from surface reactions with specifically adsorbing ions.

Colloids in the Aquatic Environment

Many colloids are contaminants; thus the presence and transport of colloids in the aquatic environment is of concern to hydrologists, environmental engineers, and public-health officials. Viruses, bacteria and asbestos particles are examples of colloidal contaminants. Colloids may also facilitate the transport of contaminants through sorption phenomena. Facilitated transport of contaminants sorbed to suspended particles has received recent attention. The high surface area per unit mass of suspended particles creates a great capacity for adsorption of many contaminants, and the hydrophobic nature of some suspended particles presents a significant sorption capacity for hydrophobic contaminants. In laboratory batch

experiments, *Gschwend and Wu [1985]* observed PCB sorption to suspended soil particles. In column experiments, *Vinten et al. [1983]* demonstrated vertical transport of DDT and paraquat sorbed to sewage effluent and suspended clay particles, respectively. It is probably safe to assume that some of the observed sorption to suspended particles in these two studies included sorption to colloids. In analyzing an extensive data set of trace metal, radioisotope and organic compound sorption, *O'Conner and Connolly [1980]* found an inverse relationship between sorption coefficients and solids concentration. Because sorption coefficients should be constant with changes in solids concentrations when all other factors are held constant, the results suggest that experimental artifacts were responsible for the noted behavior. Contaminant sorption to suspended particles, including colloids, coupled with inadequate phase separation, is implicated.

Viruses are one category of colloids that pose a particularly distinct threat to ground-water quality. Pathogenic viruses can enter ground water from a number of sources such as septic tanks, cesspools, sewage lagoons, sludge drying beds, leaky sewer lines, waste dumps, and land subjected to wastewater application. Once introduced, viruses can travel hundreds of meters in ground water and remain infective [*Yates et al., 1987*]. The danger cannot be ignored; one virus particle is capable of establishing infection in a mammalian host [*Westwood and Sattar, 1976*]. *Craun [1979]* cites evidence that almost half of the waterborne disease outbreaks in the U.S. during the period 1971-1977 were caused by consumption of contaminated ground water. But the importance of understanding virus transport in ground water is not limited to water-quality issues; understanding virus transport in ground water can increase our understanding of colloid transport in general. Viruses have been used as model colloids because they are easy to enumerate

and they have a uniform size distribution. Different species range in size from 20 to over 100 nm in diameter and have a variety of hydrophobic and isoelectric characteristics, allowing researchers to study a range of colloid properties. Also, many virus surfaces have been or can easily be characterized.

Virus Transport in Ground Water

Virus fate in ground water is thought to be governed by sorption to immobile substrates and by inactivation [*Yates et al., 1987*]. In a study of over one hundred ground water samples, *Yates et al.* [*1985*] found temperature to be the only measured water characteristic significantly correlated with viral inactivation. *Gerba* [*1984*] cites extensive evidence to the effect that sorbed viruses are generally protected from inactivation relative to free viruses. Virus inactivation is thought to be a first-order reaction [*Hurst et al., 1980*; *Reddy et al., 1981*; *Yates et al., 1985*].

Virus sorption is a function of physical and chemical forces and the numerous factors that affect these forces. Van der Waals forces, electrostatic double-layer forces, specific chemical interactions and hydrophobic effects appear to be the primary forces involved in colloid sorption.

Van der Waals forces are attractive physical forces between neutral molecules. They are thought to consist of three types of forces. One set of these forces arise from mutual orientation of pairs of molecules with permanent dipoles such that attraction results. Another set of forces arise when dipolar molecules induce dipoles in other molecules; again, attraction results. Lastly, intermolecular attractive forces known as London-van der Waals forces arise when polarization of non-polar molecules by charge-distribution fluctuations in other non-polar molecules results in attraction.

London-van der Waals forces are the dominant forces in van der Waals forces except in the case of highly-polar materials. The energy of attraction between two molecules follows an inverse sixth power law with respect to inter-molecular distance over short distances. For colloids, London-van der Waals forces are approximately additive. Empirical equations approximating London-van der Waals forces between colloids are described by *Schenkel and Kitchener [1960]*, *Ho and Higuchi [1968]*, *Rajagopalan and Kim [1981]*, and others. Equations given by *Ho and Higuchi [1968]* approximating London-van der Waals forces between unequal spherical colloids are:

$$V = -\frac{Aa_1a_2}{6(a_1+a_2)H}\frac{\lambda}{\lambda+11.116H} \qquad 0<p<2, \quad H \ll a_1, a_2 \quad (1)$$

$$V = \frac{Aa_1a_2}{a_1+a_2}\left\{-\frac{2.45\lambda}{60\pi H^2}+\frac{2.17\lambda^2}{360\pi^2H^3}-\frac{0.59\lambda^3}{1680\pi^3H^4}\right\} \qquad p>0.5, \quad H \ll a_1, a_2 \quad (2)$$

where

V = attractive potential between unequal spherical colloids,

A = Hamaker constant,

a_1, a_2 = particle radii,

H = shortest particle separation distance,

$p = 2\pi H/\lambda$, and

λ = London wave length, the wavelength corresponding to the intrinsic electronic oscillations of the atoms; generally $\lambda \approx 100$ nm.

Double-layer theory holds that charged particles in aqueous solutions attract counterions from the surrounding solution. These counterions form a tightly

bound layer near the surface, called the Stern layer; ions in the Stern layer partially neutralize the surface charge and can even reverse the surface charge. A less-tightly bound layer of counterions extends beyond the Stern layer; it is generally refered to as the Gouy layer or the diffuse layer. The double layer consists of the combined Stern and diffuse layers. Attractive or repulsive electrostatic forces between particle double layers constitute double-layer forces. Stern-layer charge and double-layer thickness determine the magnitude of double-layer forces. Double-layer thickness is a function of the ionic strength of the suspending solution. The charge of an amphoteric surface, and thus the charge of the Stern layer of most colloids, varies with solution pH. The Stern layer is thought to lie inside the plane of shear and it is generally assumed that the potential at the Stern layer is determined when colloid surface potential is calculated from electrophoretic mobility.

Colloid sorption is a function of the frequency of colloid collisions with immobile substrates and the sticking efficiency of those collisions. Collision frequency in saturated porous media is determined by Brownian motion and convective transport. Sticking efficiency is a function of the attractive and repulsive forces between particles. Derjagin and Landau, and Verwey and Overbeek, independently developed a colloid stability theory for like-charged surfaces, now known as the DLVO theory. DLVO theory holds that colloid stability is governed by the sum of attractive van der Waals forces and repulsive double-layer forces [*Verwey and Overbeek, 1948*].

Murray and Parks [*1980*] conducted batch experiments with poliovirus as the sorbate and a variety of metal oxides as sorbents. Experimentally determined free energies of adsorption were found to correspond well with potentials

predicted by DLVO theory. Other contributions to the free energy of adsorption were considered; these included configurational entropy, dehydration energy, electrostatic induction potentials, covalent-ionic interactions, hydrogen bonding, and hydrophobicity. None appeared to be important in their system.

Although DLVO theory appears to explain poliovirus adsorption to metal oxides, it fails to account for interactions that may be important sorption mechanisms in other systems. Purely chemical interactions may contribute to colloid sorption. For instance, divalent cations were shown to be more effective than monovalent cations in promoting adsorption of poliovirus to membrane filters [*Wallis and Melnick, 1967*]. *Mix* [*1974*] proposed that cations may act as complexing agents in sorption, forming salt bridges between viruses and surfaces.

Hydrophobic effects may also be important in some environments. Hydrophobic interactions arise because the nonpolar nature of many organic substances disturbs the structure of polar solvents such as water [*Kauzmann, 1959*; *Stumm and Morgan, 1981*]. Solvation of nonpolar substances in polar solvents increases the net free energy of a system. Differences in free energy in such systems result in a driving force often referred to as a hydrophobic effect. Sorption of nonpolar organic substances onto surfaces may be driven, in part, by hydrophobic effects. Colloid sorption onto or into an organic phase may occur when organic matter is present in an aquatic environment; organic matter charge and identity, organic matter surface area, and total fraction of organic carbon all have an effect on hydrophobic partitioning. Colloid sorption may also occur in a carbon-free environment; such sorption can be driven by a lower free energy for a colloid on a surface than in an aqueous solution.

Batch experiments with bacteriophage ΦX174 and five different soils showed a strong correlation between sorption and organic carbon content [*Burge and Enkiri, 1978*]. Other studies focusing on the role of organic carbon content on colloid sorption are noticeably lacking.

Farrah and coworkers attempted to shed some light on the role of hydrophobicity in virus sorption by studying the effects of chaotropic and antichaotropic salts on the elution of sorbed viruses. Chaotropic agents disrupt the structure of water, and antichaotropic agents increase the structure of water. Thus chaotropic salts should reduce the hydrophobic component of a sorption potential, while antichaotropic salts would be expected to produce the opposite effect. Chaotropic and antichaotropic salts had no effect upon elution of poliovirus from membrane filters at low pH, but at high pH, antichaotropic salts retarded or prevented elution of viruses from membrane filters. Furthermore, chaotropic salts antagonized the effects of antichaotropic salts at high pH [*Farrah et al., 1981*]. These results led the investigators to conclude that electrostatic interactions dominate in poliovirus sorption to membrane filters at low pH (pH 4), but that hydrophobic interactions dominate at high pH (pH 9). Similar results were also found with bacteriophage MS2 [*Farrah, 1982*]. One should ask, however, if these changes in sorption were in fact due to a hydrophobic effect, or if the chaotropic and antichaotropic salts altered the surface charge of the membrane filters. Experiments conducted upon soils or beads of varying organic carbon contents would produce more definitive and quantitative results.

Colloid Transport Models

In applying quantitative techniques to the interpretation of virus sorption and transport data, the plaque-forming unit (pfu) is the standard virus concentration unit of measure, as virus plaques rather than actual viruses are counted in viral assays. A pfu is not necessarily equivalent to one virus particle, but the pfu does present a consistent means of measuring virus concentration.

Equations governing advection-dispersion solute transport are well known and can be applied to colloid transport. The basic equations and their analytical solutions are discussed in *Freeze and Cherry* [*1979*], *Bear and Verruijt* [*1987*] and elsewhere. *Van Genuchten* [*1981*] has written a nonlinear-least-squares numerical curve-fitting computer program, CFITIM, that estimates parameters for various forms of the one-dimensional advection-dispersion solute transport equation:

$$\frac{\partial C}{\partial t} + \frac{\rho}{\theta}\frac{\partial S}{\partial t} = D\frac{\partial^2 C}{\partial x^2} - v\frac{\partial C}{\partial x} \tag{3}$$

where

C = aqueous concentration (pfu cm^{-3}),

D = dispersion coefficient ($cm^2\,s^{-1}$),

S = sorbed concentration (pfu g^{-1}),

t = time (s),

v = mean pore-water velocity ($cm\,s^{-1}$),

x = distance (cm).

θ = volumetric soil-water content ($cm^3\,cm^{-3}$), and

ρ = bulk density (g cm^{-3}).

Equation 3 expresses solute concentration change with time due to advection and dispersion. Equation 3 is based upon several assumptions: flow occurs under steady-state conditions and is governed by Darcy's Law, the medium is homogeneous and saturated with a constant soil-water content, immobile flow regions do not exist, and known relationships between sorbed and aqueous solute concentrations exist.

I have chosen to use two of the four-parameter models in CFITIM [*Van Genuchten 1981*] to aid in the interpretation of breakthrough data. The first of these models is the pseudo-first-order one-site kinetic non-equilibrium sorption model. It is based on the assumption that sorption to an immobile substrate is governed by kinetic non-equilibrium sorption. The second of these models is the pseudo-first-order two-site kinetic non-equilibrium sorption model. This model is based upon the assumption that sorption to one fraction of sorption sites does not exhibit kinetically-limited sorption while the other fraction does. The two-site model may be particularly relevant to virus sorption because virus surfaces contain a number of functional groups. These various groups have different affinities for other functional groups and surfaces, as well as different dissociation constants. The complex nature of virus surfaces may promote more than one type of sorption mechanism. In the case where all of the surface sites are identical, the two-site model collapses to the one-site kinetic non-equilibrium adsorption model. These models are developed in *Cameron and Klute* [*1977*].

In the two-site model, the following equations describe the relevant sorption relationships:

$$S_1 = FKC \tag{4}$$

$$\frac{\partial S_1}{\partial t} = FK\frac{\partial C}{\partial t} \tag{5}$$

$$\frac{\partial S_2}{\partial t} = \alpha[(1-F)KC - S_2] \tag{6}$$

$$S = S_1 + S_2 \tag{7}$$

$$\frac{\partial S}{\partial t} = \frac{\partial S_1}{\partial t} + \frac{\partial S_2}{\partial t} \tag{8}$$

where

F = fraction of sites exhibiting fast sorption,

K = distribution coefficient between solid and liquid phases ($cm^3\ g^{-1}$) and

α = pseudo-first-order desorption rate from kinetic sites (s^{-1}).

The subscripts 1 and 2 refer to fast and kinetically-limited sites, respectively. In the one-site kinetic non-equilibrium model F is equal to zero, equations 4 and 5 drop out of the set of equations, and equations 3 and 6 define transport in the system.

Dimensionless parameters used in this model are:

$$P = \frac{vL}{D} \tag{9}$$

$$R = 1 + \frac{\rho K}{\theta} \tag{10}$$

$$R_m = 1 + F\rho\frac{K}{\theta} \tag{11}$$

$$\beta = \frac{R_m}{R} = \frac{\theta + F\rho K}{\theta + \rho K} \tag{12}$$

$$\omega = \frac{\alpha(1-\beta)RL}{v} \tag{13}$$

Where P = Peclet number (dimensionless inverse coefficient of hydrodynamic dispersion),

L = column length (cm),

R = retardation factor,

R_m = retardation factor for fast sites,

β = (dimensionless) ratio of R for fast sites to R, and

ω = dimensionless first-order rate coefficient.

Dimensionless variables used in this model are:

$$T = \frac{vt}{L} \tag{14}$$

$$Z = \frac{x}{L} \tag{15}$$

$$C_1 = \frac{C}{C_0} \tag{16}$$

$$C_2 = \frac{S_2}{(1-F)KC_0} \tag{17}$$

Where

T = number of pore volumes,

Z = dimensionless length,

C_0 = input concentration (pfu cm^{-3}), and

C_1, C_2 = dimensionless concentrations.

Substitution of equations 5, 8, 9, 10, and 12 through 17 into equations 3 and 6 result in the following dimensionless equations:

$$\beta R\frac{\partial C_1}{\partial T} + (1-\beta)R\frac{\partial C_2}{\partial T} = \frac{1}{P}\frac{\partial^2 C_1}{\partial Z^2} - \frac{\partial C_1}{\partial Z} \tag{18}$$

$$(1-\beta)R\frac{\partial C_2}{\partial T} = \omega(C_1 - C_2) \tag{19}$$

The initial conditions are:

$$C_1(Z,0) = C_2(Z,0) = 0 \tag{20}$$

$$S_1(Z,0) = S_2(Z,0) = 0 \tag{21}$$

The boundary conditions are:

$$\left\{-\frac{1}{P}\frac{\partial C_1}{\partial Z} + C_1\right\}_{(0,T)} = 1 \tag{22}$$

$$\frac{\partial C_1}{\partial Z}_{(1,T)} = 0 \tag{23}$$

Equation 23 is strictly valid only for an infinite column, but appears to closely approximate the lower boundary condition in finite columns; see, for instance, *van Genuchten and Wierenga, 1976.*

Equations 18 and 19 have been well studied and analytical solutions for these or similar equations subject to various initial and boundary conditions are well known; see, for example, *Coates and Smith [1964]*, *Cameron and Klute [1977]*, and *Popovic and Deckwer [1976]*.

Research Objectives

Few colloid transport experiments conducted to date have involved well-characterized surfaces; as a result, most of the information obtained has been qualitative in nature. Desorption data have, in particular, been ignored. A number of mathematical models and solution techniques for colloid transport are available. It has been proposed that current modeling efforts are limited by a lack of quantitative data for model validation [*Yates et al., 1987*]. The purpose of this research was to attempt to obtain quantitative information on virus transport for model validation. Column experiments with well-characterized bacteriophage and silica surfaces were conducted in order to study the contributions of pH and kinetics to colloid transport.

MATERIALS AND METHODS

Four controlled laboratory continuous-flow column experiments were conducted to determine the influence of pH and kinetics on the transport of bacteriophage PRD1. Columns were packed with well-characterized silica beads. Adsorption experiments were conducted at pH 5.5 and pH 7.0. Phage sorbed at pH 5.5 were eluted with buffers at elevated pH to gain a better understanding of the role of pH changes in colloid desorption and transport. Temperature was maintained at 4°C in these experiments in order to minimize viral inactivation.

Column-Experiment Procedure

The column experiment apparatus set-up is illustrated in Figure 1. All column experiments were conducted at 4°C in a 15-cm x 0.9-cm inside-diameter precision-bore-glass chromotography column (Spectrum Medical Industries, Inc., Los Angeles, CA). All column fittings were made of teflon. Buffers and phage were stored in glass reservoirs and fed through the flow system by an Ismatec peristaltic pump (Cole Parmer Instrument Co., Chicago, IL). Teflon tubing was used everywhere in the flow system except in the peristaltic pump, where flexible Tygon peristaltic tubing (Cole Parmer Instrument Co.) was used. In all column experiments, phage were pumped through the peristaltic tubing for a minimum of 18 hours prior to the begining of an experiment. Column packing was performed by the tap and fill method of *Snyder and Kirkland* [*1979*]. Columns were packed with new beads for each experiment, with the exception of column experiment 2, which was used following experiment 1 because no adsorption had occurred in experiment 1 and the pH conditions were identical. Column flooding was performed with buffer of pH 7 (experiments 1 and 2) or pH 5.5 (experiments 3 and 4).

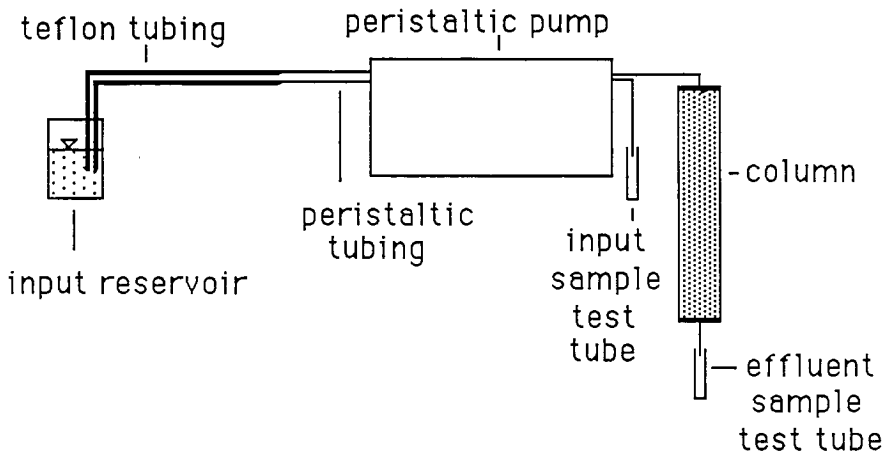

Figure 1. Column experiment apparatus

After slow overnight flooding from the bottom to remove air, the column was flooded from the top with a minimum of 100 pore volumes of buffer prior to the beginning of an experiment.

Reservoir phage were routed through two sets of identical tubing consisting of teflon tubing in the reservoir leading to and attached directly to the peristaltic tubing that led through the pump to the column setup. One tube was used to feed the column, while the second lead to a waste container. Reservoir samples were taken from the end of the second tube so that any phage loss to the peristaltic tubing was accounted for. Reservoir samples were taken during the length of the adsorption phase of the experiments in order to detect inactivation that may have been present, but titres remained constant, within experimental error. Samples were collected in sterile glass test tubes for a period of 15 to 20 minutes per sample and were assayed the same day they were collected. The first sample was always taken before the experiment began; the last, after the adsorption phase ceased. A minimum of seven reservoir samples were taken in one-day experiments (experiments 1 and 2), and a minimum of ten for multiple-day experiments (experiments 3 and 4). Titres used ranged from 0.9 to 3.9×10^{-5} pfu ml^{-1}.

Desorption solutions were fed to the column with separate, uncontaminated tubing. Column effluent samples were collected in sterile glass test tubes at various times during the experiment for a period of 10 to 15 minutes per sample. All samples were assayed on the same day they were taken, with the exception of one sample in experiment 3 that was taken late in the night and analyzed the following morning. pH of all influent solutions was measured prior to the experiments, and effluent pH was measured during the course of the experiments. pH did not vary by more than ± 0.06 pH units from target pH values, with the exception of

the pH 8 and 9 Tween-80-detergent and beef-extract eluent phases of experiment 4, when pH values dropped from pH 8.00 to pH 7.86, and from pH 9.00 to 8.81. It is possible that the eluents were involved in surface-chemical reactions that released acid into solution. Few phage were eluted in these phases, so the lack of pH control was not cause for concern.

Sorption experiments were carried out with calcium-phosphate buffer at pH 7 (column experiments 1 and 2) and pH 5.5 (column experiments 3 and 4). Sorption occurred in experiments 3 and 4, so sorption was followed by a sequential desorption process. In experiment 3, desorption was initiated with calcium-phosphate buffer at pH 5.5 and followed by calcium-free phosphate buffer at elevated pH (pH 7). Two variables (calcium and pH) were varied simultaneously in this desorption step. Desorption was concluded by desorption with calcium-free phosphate buffer at pH 7 with 1% beef extract. In experiment 4, desorption was initiated as in experiment 3, with calcium-phosphate buffer at pH 5.5. In order to better identify the factors contributing to desorption, desorption was continued with calcium-free phosphate buffer at pH 5.5, followed by calcium-free phosphate buffer at elevated pH (pH 8). In an effort to obtain more complete desorption, desorption was continued with calcium-free phosphate buffer at pH 8 with 1% Tween 80 detergent and 2.5% beef extract, followed by desorption with identical buffer at pH 9. In experiments 1, 2 and 4, calcium, when present, was present at 10^{-6} M; in experiment 3, calcium, when present, was present at 10^{-4} M.

Flow rates were monitored continuously during experiments. Flow rates corresponded to 64 minutes per pore volume in all column experiments except in experiment 2, where pore volumes averaging 94 minutes were used in an unsuccessful attempt to induce adsorption. Flow rates remained fairly steady most of

the time but did occasionally change by as much as ± 9.5% before recovery to rates close to targeted rates. Effective column pore volumes were calculated following completion of column experiments by characterizing conservative tracer breakthrough as follows. Columns were flooded with 0.01 M NaCl overnight. A 0.03 M NaCl solution was introduced and the conductivity of the column outflow monitored with a Wescan model 213a conductivity detector (Wescan Instruments, Inc., Santa Clara, CA) connected to a Miniservo strip-chart recorder model MS401BB (Esterline Angus Instrument Corp., Indianapolis, IA) or a flat-bed recorder series L6512 (Linseis, Inc., Marina Del Rey, CA). Flow rates were also monitored. Upon stabilization of conductivity readings, 0.01 M NaCl was again introduced at the top of the column while conductivity and flow rate continued to be monitored. The product of the average of the two breakthrough times (corrected for column dead space) with the average flow rate gave the effective column pore volume (ml per pore volume) for a conservative tracer in that particular column packing. With this conversion factor, flow rates measured during the course of a column experiment were converted from units of ml per minute to pore volumes per minute. Pore volumes calculated by conservative tracer breakthrough were greater than pore volumes calculated volumetrically by as much as 4.6%. This large error may be due in part to variability in bead specific gravity measurements. Technical data provided with the beads reports their specific gravity as 2.45 to 2.50 g cm^{-3}. In my volumetric calculations, I assumed a density of 2.475 g cm^{-3}; a density of 2.50 g cm^{-3} would reduce the discrepency in pore volume calculations to less than 3%.

Media

Trypticase soy broth (TSB) host medium was prepared by dissolving, with the application of heat, 30 g of Tryptic soy broth powder (Gibco Laboratories, Madison, WI; Difco Laboratories, Detroit, MI) in 1 l of distilled water. Three-ml and 100-ml aliquots of TSB were then dispensed into glass test tubes and glass erlenmeyer flasks, respectfully; these were capped, sterilized by autoclaving for 20 minutes, and stored at 4°C.

Trypticase soy agar (TSA) overlay medium was prepared by dissolving, with the application of heat, 30 g of TSB powder and 10 g of bactoagar (Difco Laboratories, Detroit, MI) in 1 l of distilled water. Three-ml aliquots were delivered into 14-ml glass test tubes; these were then capped, autoclaved for 20 minutes, and stored at 4°C.

TSA plates for phage growth and assay were prepared by dissolving, with the application of heat, 40 g of tryptic soy agar (Gibco laboratories, Madison, WI; Difco Laboratories, Detroit, MI) in 1 l of distilled water. This solution was then autoclaved for 20 minutes, cooled to 50°C, and dispensed in 10-ml aliquots into sterile, 100-mm by 15-mm plastic petri dishes (Becton Dickinson Co., Lincoln Park, NJ). TSA plates were cooled overnight and stored at 4°C in their original plastic bags.

Phosphate buffers were made with $NaH_2PO_4 \cdot H_2O$ and Na_2HPO_4. pH 5.5, 0.02 M phosphate buffer was made with 2.6700 g l^{-1} of $NaH_2PO_4 \cdot H_2O$ and 0.0925 g l^{-1} of Na_2HPO_4. The proportions for pH 7.0 phosphate buffer were 1.2971 g l^{-1} and 1.5052 g l^{-1}, respectively. Buffer crystals were added to a sterile one-liter volumetric flask to which deionized water was added to the one-liter mark.

Calcium-phosphate buffers were made in a similar manner. Buffer crystals, measured volumes of concentrated calcium solution, and deionized water were added to the one-liter mark. Ten ml l^{-1} of a 10^{-2} M $CaCl_2$ solution was used in 10^{-4} M calcium buffers and 1.00 ml l^{-1} of a 10^{-3} M $CaCl_2$ solution in 10^{-6} M calcium buffers. In an unsuccessful attempt to promote adsorption in the first two column experiments, the ionic strength of those pH 7 buffers was elevated by adding 4.6752 g l^{-1} of NaCl (0.08 M NaCl) along with the phosphate salts. If necessary, pH was adjusted with concentrated HCl and NaOH, but the quantities of acid and base needed were on the order of microliters. pH 7.3 calcium-phosphate buffer for PRD1 harvesting, and pH 8 phosphate buffer for virus elution in experiment 4, were made by adjusting the pH of lower-pH buffers with concentrated NaOH and HCl. High-pH buffers containing beef extract and detergent were also made; Tween 80 detergent [*Farrah et al., 1981*] and beef extract [*Berg et al., 1968*] have been successfully used in virus elution. Deionized water was added to appropriate amounts of beef extract V (Becton Dickinson and Co., Cockeysville, MD) and/or polyoxyethylene (20) sorbitan monooleate (Tween 80) (J.T. Baker, Inc., Phillipsburg, NJ) to yield 1.0% or 2.5% solutions. These solutions were autoclaved for 20 minutes, cooled to 4°C, added to sterile 100-ml volumetric flasks each containing 0.2840 g of Na_2HPO_4, stirred with sterile magnetic stir bars, cooled again, and adjusted to an appropriate pH with concentrated NaOH and HCl. pH values of all buffers were always rechecked before use in experiments.

Tris buffered saline solution (TBSS) was prepared by dissolving 63.2 grams trisma base (Sigma Chemical Co., St. Louis, MO), 163.6 g NaCl, 7.46 g KCl,and 1.13 g Na_2HPO_4 in 1600 ml of distilled water. The solution was stirred with a magnetic stir bar and the pH was adjusted to between pH 7.2 and 7.4 by addition

of concentrated HCl. Thirty-two ml of TBSS was added to 368 ml of distilled water; this solution (Tris) was stirred with a magnetic stir bar, autoclaved for 20 minutes, distributed with a sterile Cornwall pipette in 2.7-ml aliquots into sterile glass test tubes, capped with sterile rubber stoppers, and stored at 4°C.

Host

PRD1 host bacteria, Salmonella typhimurium LT2, was prepared as follows. From University of Arizona Department of Microbiology and Immunology stock cultures or existing plate cultures, an individual bacteria colony was spread on a TSA plate with a flame-sterilized wire loop and incubated at 37°C overnight. Spread plates were then stored at 4°C for future use. New spread plates were made every two to four weeks. Cultures for phage growth or assay were prepared by inoculating test tubes containing 3 ml of TSB with one to three isolated bacteria colonies; again, a flame-sterilized wire loop was used to transfer the bacteria. The cultures were then incubated at 37°C overnight.

Assay Procedure

Two to 3 hours before an assay, a 3-ml host culture was removed from the incubator, added to a 100-ml flask of TSB, and placed on a 37°C shaker table for 2 to 3 hours to bring growth to log phase. TSA plates were warmed to room temperature. Overlay media tubes were warmed to 49°C in a water bath.

Samples to be assayed were diluted to appropriate concentrations, usually 10 to 300 PFU per 0.1 ml. Glass pipettes were used in all phage work. Dilutions were carried out in either tris or fresh pH 5.5 calcium-phosphate buffer; in any given column experiment, one dilution medium was used for consistency. Sequential

dilutions were made by pipetting 0.3 ml of dilutant into 2.7 ml of tris or buffer and vortexing the mixture for 5 seconds. One ml of host culture and 0.1 ml of appropriately diluted sample were added to each of between two and six overlay media tubes. These solutions were vortexed for five seconds, after which the contents were poured onto TSA plates and allowed to solidify for 15 to 30 minutes. The plates were incubated overnight and at that point individual plaques were counted with a C-100 automatic plaque counter (New Brunswick Scientific Co., New Brunswick, NJ).

Phage

Bacteriophage PRD1 is an icosahedral lipid phage with a diameter of 62 nm [*Olsen et al., 1974*]. PRD1 was obtained from Jui-Cheng Hsieh (Department of Microbiology and Immunology, College of Medicine, University of Arizona, Tucson). Phage were grown and purified for experiments using many of the steps discussed in the assay procedure section above. Twenty-five to 50 TSA plates were prepared with confluent plaques (approximately 10^4 plaques per plate). PRD1 was harvested by dispensing 10 ml of pH 7.3 calcium-phosphate buffer onto each plate. Plates remained at room temperature for two hours and were then agitated by hand, and the eluent was poured into 250-ml polypropylene centrifuge bottles. The eluent solutions were centrifuged at 10,000 rpm for 10 minutes in a Beckman JC-21 centrifuge (Beckman Instruments, Irvine, CA) and removed, leaving behind an agar pellet. Bacteria fragments were removed by filtration through a 0.45-μm membrane filter (Millipore Corporation, Bedford, MA). The phage solution was then purified by ultracentrifugation at 25,000 rpm for 93 minutes in a Beckman L8-70 ultracentrifuge. The supernatent, containing bacteria fragments and media

residues which are less dense than phage, was discarded. The phage pellet was resuspended in buffer by pipetting action, and the concentrated phage was removed and diluted in 10 ml of buffer. As an added precaution, the PRD1 stock was filter sterilized through a 0.20-μm membrane filter (Corning Glass Works, Corning, N.Y.). Phage titres between 10^{11} and 10^{13} pfu ml^{-1} were obtained. For microelectrophoretic experiments, PRD1 was further purified in a sucrose gradient. Concentrated PRD1 stock was placed at the top of a series of filter-sterilized sucrose solution bands made of 20%, 10% and 5% sucrose by weight in deionized water. The gradients were placed in a Beckman L8-70 ultra-centrifuge for 105 minutes at 45,000 rpm, after which the pellet was resuspended in 1 ml of buffer. A titre of approximately 10^{12} pfu ml^{-1} was obtained.

Silica

Spheriglass 2530 silica beads (Potters Industries, Inc., Hasbrouck Heights, NJ) were used for sorption surfaces. These beads contained soluble oxides of calcium and sodium that had to be removed from the surfaces before use in column experiments. One-hundred-ml volumes of beads (approximately 140 g) were rinsed in deionized water, rinsed in 500 ml of 1 M NH_4OH, and rinsed in deionized water until the pH of the rinse water dropped below pH 11. Beads were then refluxed in 500 ml of 2 M HCl for 4 hours, rinsed in deionized water, and refluxed in fresh 2 M HCl for 2 more hours. The HCl was drained and replaced with fresh 2 M HCl and refluxed another 2 hours. The beads were next rinsed in deionized water until the rinse-water pH rose above pH 4. The beads were next refluxed in deionized water for one hour in order to remove excess hydrogen ions from the surfaces. It was found in preliminary microelectrophoresis work that beads refluxed in acid

and not refluxed in water held a nearly-neutral surface charges that only slowly reached equilibrium with solutions. Finally the beads were rinsed in deionized water and then oven dried overnight at temperatures never exceeding 200°C.

Silica surface area was determined by single-point N_2 adsorption on a model QS-10 Quantasorb Sorption System (Quantachrome Corp., NY). Surface areas for the silica beads were 0.0604 ± 0.0082 m^2g^{-1} and 0.0665 ± 0.0056 m^2g^{-1} for two sets of beads. Only conventional adsorption cells (cell #100, Quantachrome Corp., NY) were available; conventional cells generally yield accurate surface area determinations for materials with surface areas over 0.2000 m^2g^{-1}, hence these surface area determinations are suspect and should only be used as rough estimates.

Silica was analyzed by Desert Analytics (Tucson, AZ) for fraction organic carbon (f_{oc}) using the elemental pyrolysis method. The f_{oc} for both batches of silica beads was 0.00002; the instrument error was $\pm$ 0.00005.

All silica was stored dry in sterile glass jars with solid PTFE stoppers.

Microelectrophoresis

A Rank Brothers Mark II particle-electrophoresis apparatus (Rank Brothers, Ltd., Cambridge, England) was used to determine particle mobility. For phage work, a cylindrical cell and a He-Ne laser (Scientifica-Cook, Ltd, London, England) were used. Small Latex beads of 80 nm diameter and known concentration (Polysciences, Inc., Warrington, PA) were used to adjust the apparatus to optimal working conditions and to estimate the ideal concentration of particles needed to insure successful mobility determination. If too few particles are present, mobility determinations are time consuming, resulting in cell overheating, or are impossible

altogether. If too many particles are present, tracking individual particles becomes difficult and particle-particle interactions may become significant. An ideal concentration of Latex beads was found to be on the order of 10^{10} beads per ml. Sucrose-gradient-purified PRD1 was suspended in calcium-phosphate buffer (10^{-4} M calcium) to yield a concentration of approximately 1.5×10^{10} pfu ml^{-1}; this concentration was found to yield excellent results.

For silica work, a flat cell and an incandescent lamp were used. Because of the large size of the silica beads, mobility determinations required an involved particle suspension process. Small beads (Spheriglass 2900; Potters Industries, Inc., Hasbrouck Heights, NJ) were washed by the same process as the larger beads. These beads were of a wide range of sizes smaller than 53 μm in diameter and they contained colloidal sized silica particles. Twenty g of washed product was placed in 1.2 l of phosphate buffer and allowed to settle. Supernatent containing suspended particles was removed and used to measure bead mobility under calcium-free conditions. Also removed was 499.5 ml of supernatent, which was combined with 0.5 ml of calcium-phosphate buffer (0.1 M Calcium), yielding a calcium-phosphate buffer with 10^{-4} M calcium. This mixture was used to measure bead mobility in the presence of calcium. Surface potentials calculated from the mobility of colloidal-sized beads was assumed equal to the surface potentials of the larger beads. Buffer pH was systematically changed with HCl and NaOH in order to obtain curves of phage and silica mobility as a function of pH.

Modeling

The analytical solution to equations 18 and 19 subject to the initial and boundary conditions of equations 20 through 23 is fit by nonlinear-least-squares to an experimentally-derived breakthrough curve. Because four parameters are unknown, solutions are not unique, but by varying parameters one at a time it is possible to qualitatively estimate to which of the parameters the system is sensitive or insensitive. When experimental variability is significant, the results of such modeling are far from definitive, but it is often possible to deduce valid order of magnitude parameter values.

RESULTS

Microelectrophoresis

PRD1 electrophoretic mobility as a function of pH in calcium-phosphate buffer (10^{-4} M calcium) is shown in Figure 2. PRD1 is negatively-charged at natural-water pH values when calcium concentrations are low.

The surface potential of the silica beads used in our column was assumed to equal the surface potential of the fine beads measured in our electrophoretic mobility apparatus. Electrophoretic mobility curves for small beads in calcium-phosphate buffer (10^{-4} M) and calcium-free phosphate buffer are shown in Figure 3. The two curves show no obvious differences in mobility, suggesting that bead surface charge is not significantly affected by the presence of calcium.

A quick calculation suggests that the beads in the 10^{-4} M calcium buffer in the microelectrophoresis experiments were probably saturated with calcium ions. Assuming a bead density of 2.5 g cm^{-3} and a mean bead diameter of 2 μm — reasonable based upon personal experience in previous microelectrophoresis work with silica powder in this size range — the surface area of the beads can be estimated to be 1.2×10^{18} nm^2 g^{-1}. One can estimate that the beads have 4.6 silanol groups (bonding sites) per square nm of silica [see *Iler, 1979*]. Assuming now a solid to liquid ratio of no more than 50 mg of silica per 500 ml of buffer — reasonable based upon personal experience in previous microelectrophoresis work and observations of the enormous mass of silica beads removed from solution vs. remaining suspended in solution before addition of calcium — the following calculation suggests a value of at least 110 for the ratio of calcium ions to bonding sites for silica beads in phosphate buffer with 10^{-4} M calcium:

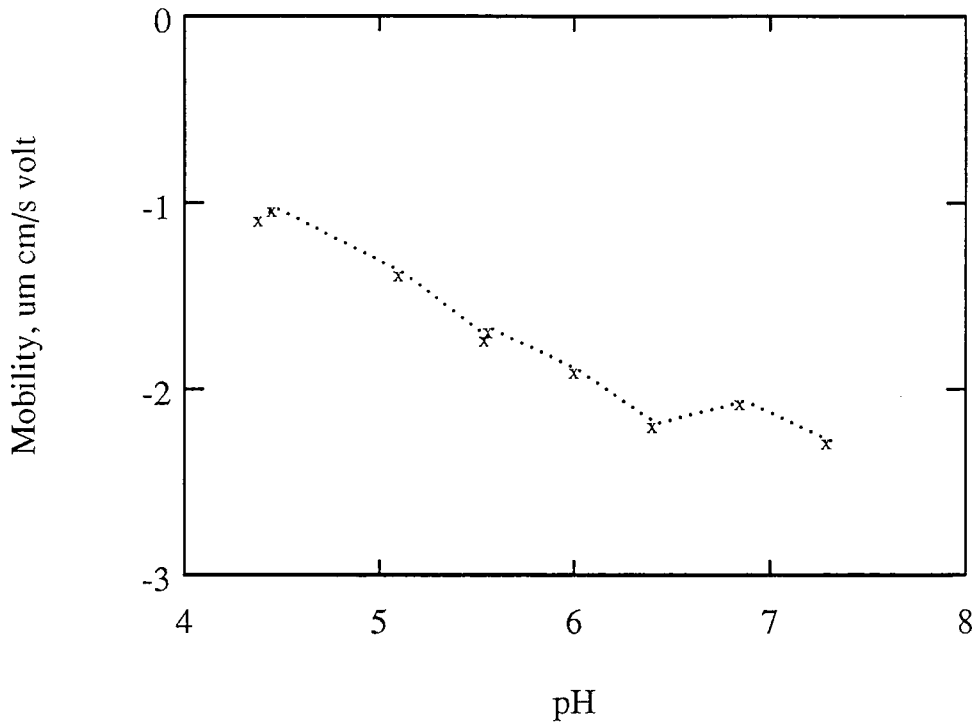

Figure 2: Mobility of PRD1 as a function of pH in phosphate buffer with 10^{-4} M calcium.

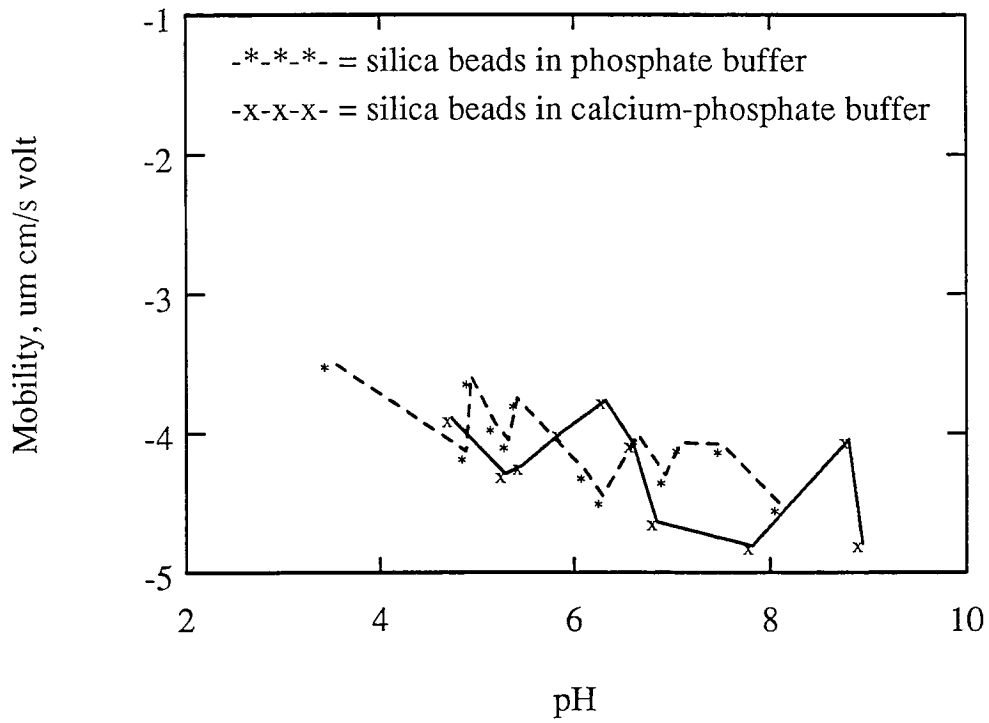

Figure 3: Mobility of silica beads as a function of pH in phosphate buffer both with 10^{-4} M calcium and without calcium.

$$\frac{0.05\ g\ SiO_2}{500\ ml\ buffer} \times \frac{1000\ ml\ buffer}{10^{-4} mole\ Ca^{2+}} \times \frac{1\ mole\ Ca^{2+}}{6.02\times10^{23} Ca^{2+}\ ions} \times \frac{4.6\ sites}{nm^2} \times \frac{1.2\times10^{18} nm^2}{g\ SiO_2} = \frac{onesite}{110\ Ca^{2+}\ ions}$$

Kinetics and pH

Figure 4 shows the breakthrough curves for column experiments 1 and 2: PRD1 transport at pH 7 in calcium-phosphate buffer (10^{-6} M calcium) at 64-minute and 94-minute pore volumes, respectively. PRD1 did not sorb at this pH; because of the apparent lack of sorption, the advection-dispersion equation was applied to the 64-minute breakthrough curve to calculate a value of P for our system.

Figure 5 shows the breakthrough curve for column experiment 3. Experiment 3 consisted of PRD1 transport at pH 5.5 in calcium-phosphate buffer (10^{-4} M calcium) at 64-minute pore volumes. Adsorption data were more variable than desorption data, possibly due to effects of virus clumping during the adsorption phase of the experiment. The slow rising limb of adsorption and the long tailing during desorption indicate kinetic nonequilibrium, strong adsorption and slow desorption. A virus pulse occurred with pH 7 eluent and no calcium; the value of C/C_0 rose to over 14. A smaller, secondary pulse occurred when 1% beef extract was used as an eluent. Mass-balance calculations indicate that 82% of sorbed phage were eluted during desorption. The lack of mass balance might have been a result of inactivation, presence of an irreversibly-sorbed component, or insufficient desorption time. Phage were still detaching after 77 pore volumes of desorption, but it is unclear whether or not complete desorption would have eventually occurred if the experiment had been run longer. More importantly, it is unclear whether or

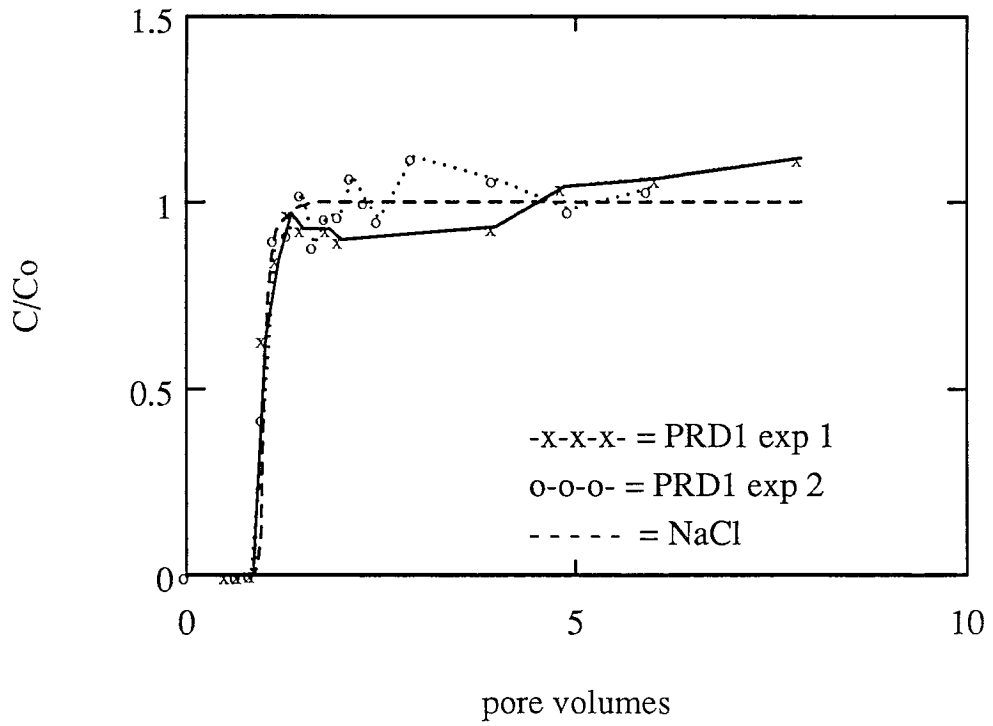

Figure 4: Breakthrough curve for column experiments 1 and 2: PRD1 breakthrough at pH 7, 64-minute and 94-minute pore volumes respectively, and conservative tracer breakthrough at 64-minute pore volumes for comparison. The phage behaved as a conservative tracer.

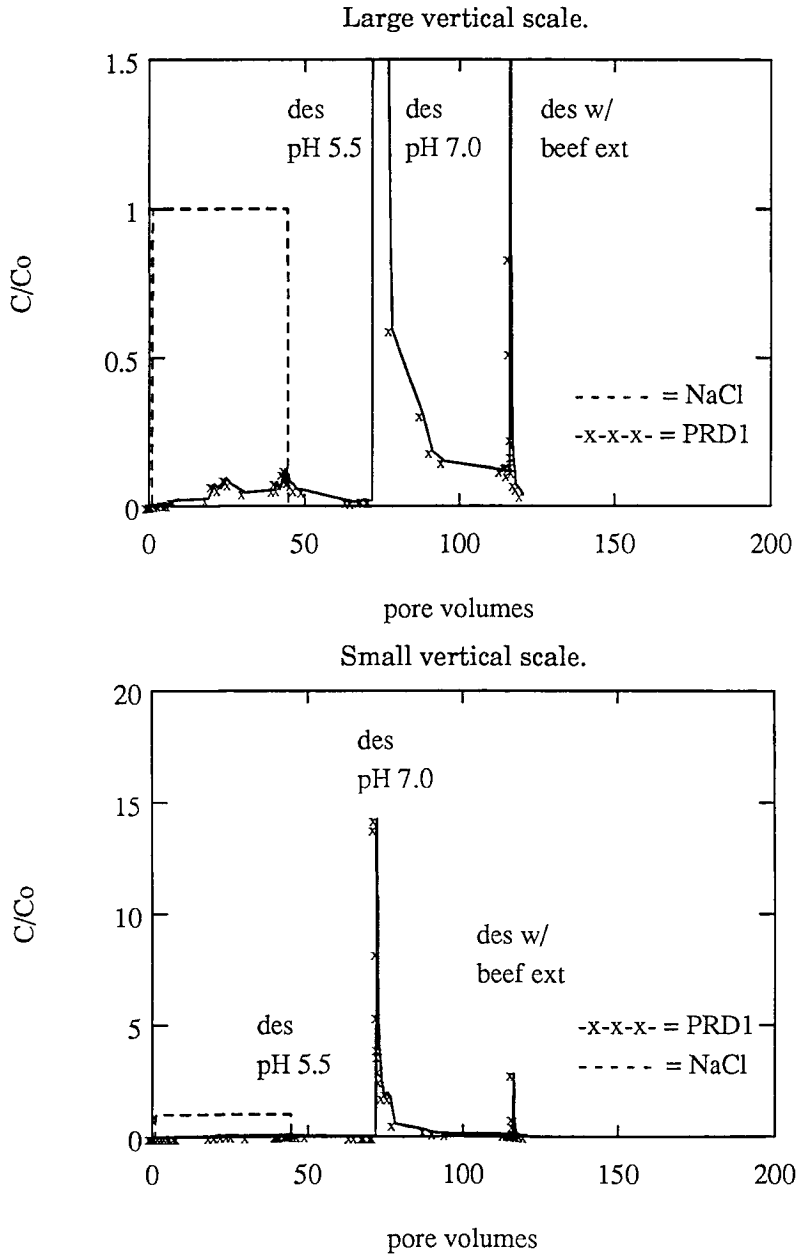

Figure 5: Breakthrough curve for column experiment 3. Adsorption was conducted at pH 5.5 with PRD1 suspended in phosphate buffer with 10^{-4} M calcium. Desorption was initiated with pH 5.5 phosphate buffer with 10^{-4} M calcium, followed by desorption with pH 7 calcium-free phosphate buffer, and ending with pH 7 calcium-free phosphate buffer with 1% beef extract. A flow rate of 64 minutes per pore volume was maintained. The conservative tracer break through is shown for comparison. The phage sorbed strongly and desorbed very slowly until the ambient pH was raised. At that time, C/C_0 rose sharply. A later and smaller desorption pulse occured with beef extract.

not, given enough time, complete desorption would have occurred at pH 5.5.

Figure 6 shows the breakthrough curve for column experiment 4. Column experiment 4 was similar to experiment 3 in that pH was maintained at 5.5, but the concentration of calcium was 10^{-6} M and the desorption procedure involved more steps, as discussed in the section on methods. As in experiment 3, adsorption was more variable than desorption, and kinetic non-equilibrium, strong adsorption and slow desorption occurred. The smaller amount of sorption in experiment 4 vs. 3 may be due to a lower calcium concentration, but any such conclusions would be premature until such a time as these experiments can be repeated. A change of eluent at pH 5.5 from calcium buffer to calcium-free buffer did not induce additional desorption, but a change of eluent pH from pH 5.5 to 8.0 did produce a large virus pulse, suggesting that changes in pH rather than changes in calcium concentration were responsible for the large desorption pulse seen in experiment 3. The importance of pH changes in virus transport are obvious. Secondary and tertiary pulses were observed in subsequent desorption steps, but they were of minor importance. After 135 pore volumes of desorption, 76% of sorbed phage were eluted. Again, incomplete mass-balance could be a result of inactiviation, the existence of an irreversibly-sorbed component, or insufficient desorption time.

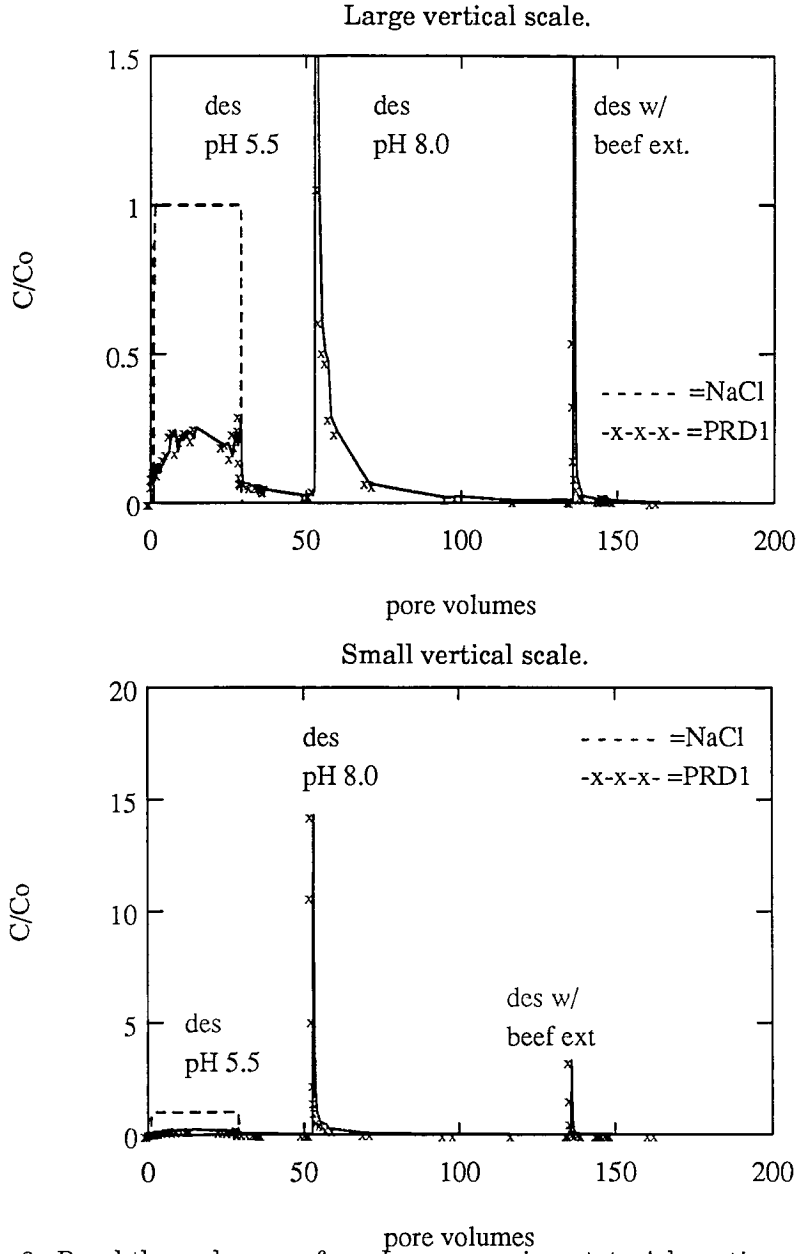

Figure 6: Breakthrough curve for column experiment 4. Adsorption was conducted at pH 5.5 with PRD1 suspended in phosphate buffer with 10^{-6} M calcium. Desorption was initiated with pH 5.5 phosphate buffer with 10^{-6} M calcium, followed by desorption with pH 5.5 calcium-free phosphate buffer, then with pH 8 phosphate buffer and ending with phosphate buffers containing 1% Tween 80 detergent and 2.5% beef extract at pH 8 and then pH 9. A flow rate of 64 minutes per pore volume was maintained. The conservative tracer break through is shown for comparison. The phage sorbed strongly and desorbed very slowly until the ambient pH was raised. At that point, C/C_o rose sharply. A later and smaller desorption pulse occured with beef extract at pH 8, but no additional phage were eluted at pH 9.

DISCUSSION

pH

The role of pH in the transport of PRD1 was demonstrated in column experiments. PRD1 sorbed strongly at pH 5.5 and was conservative at pH 7. When adsorption occured and the ambient pH of the solution was increased, large pulses of PRD1 swept through the silica columns. A phage pulse of over fourteen times initial input concentration was observed in both experiments 3 and 4 during desorption at elevated pH.

The results of this research are qualitatively consistent with DLVO theory. Strong adsorption at low pH and a lack of adsorption at high pH would be expected in a system such as this one in which both the colloids and the immobile surfaces have low isoelectric points. The desorption of sorbed phage resulting from an increase in the ambient solution pH is also consistent with DLVO theory.

The results observed in this research are also consistent with those of *Kroeger* [*1989*] and *Stocking* [*1989*]. *Kroeger* [*1989*] conducted batch experiments with bacteriophage MS2 and silica powder. MS2 adsorbed to silica at pH 5.0 but did not adsorb at pH 7.0. *Stocking* [*1989*] performed column experiments with bacteriophage MS2 and silica beads. MS2 adsorbed to silica at pH 5.0 and was eluted at pH 7.0.

Kinetics

PRD1 sorption to silica beads was kinetically controlled and occurred under nonequilibrium conditions. The distribution coefficient for PRD1 sorption to silica beads at pH 5.5 is large, yet because of nonequilibrium sorption in our column experiments, some suspended PRD1 continually migrated through the column during the adsorption phase of the experiments. Flow rates of 3.9×10^{-3} cm s^{-1}, used in our pH 5.5 experiments, would not be uncommon in groundwater flow; thus it is likely that nonequilibrium conditions would prevail in many cases of colloid transport in natural systems.

The error that can be introduced by using batch-experiment distribution coefficients in the modeling of virus transport in nonequilibrium situations becomes strikingly apparent in Figures 5 and 6. The purpose of conducting batch experiments is to obtain *equilibrium* distribution coefficients. In batch experiments, the amount of sorbent sorbed increases with time until equilibrium is attained; generally this increase approaches the equilibrium concentration asymptotically. Because changes in adsorbed sorbent become smaller with each time step, often becoming smaller than the error of measurement, determination that equilibrium has occured can be difficult. Assuming, however, that batch-experiment equilibrium distribution coefficients have been obtained under equilibrium conditions, care must be taken in their application to transport modeling. In applying equilibrium distribution coefficients to the modeling of colloid transport, the assumption is made that sorption occurs under equilibrium conditions. Under equilibrium conditions, colloids are transported through the porous medium only when sorption sites have reached saturation. Under non-equilibrium conditions, colloids may be

transported through the porous medium before site saturation is attained, as was the case in experiments 3 and 4. Obviously the improper application of equilibrium sorption parameters can lead to serious errors in the prediction of colloid transport.

The small desorption rates observed under steady-state conditions at pH 5.5 and the large desorption pulses observed upon elevating pH are of interest. It appears that chemical perturbations such as changes in pH may, in some situations, cause more desorption of colloids than would occur over long periods of time by steady-state desorption alone. On the other hand, viruses pose a health threat in even minute concentrations; a slow desorption rate under steady-state conditions could result in a long-term and dangerous release of viruses into ground water.

Modeling and parameter estimation

A best-fit breakthrough curve and a pair of bounding fits for column experiment 1 were determined by trial and error fitting of the advection-dispersion equation to the breakthrough curve of experiment 1. In solving the advection-dispersion equation, the retardation factor was held at unity because of the lack of sorption in this experiment. The results are shown in Figure 7. Figure 7a represents a reasonable fit of the data; the Peclet number (P) is 237. In Figure 7b, when P is smaller by one order of magnitude, dispersion appears to be too great; when P is larger by an order of magnitude, the curve is unreasonably sharp, that is, it begins to resemble plug flow. It appears that P for our system at a flow rate of 3.9×10^{-3} cm s^{-1} can be fairly-well estimated from this fitting, although choosing a value of 237 for P

(a) Best fit of the Peclet number to experiment 1.

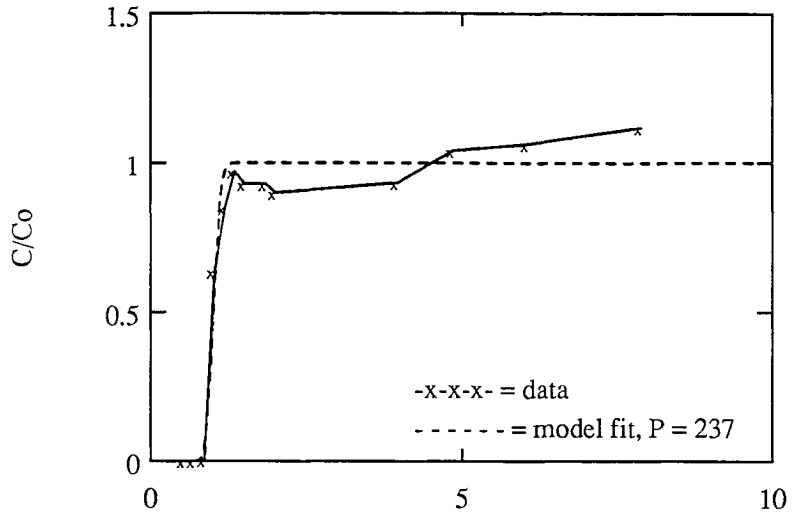

(b) High and low bounding values of the Peclet number for experiment 1.

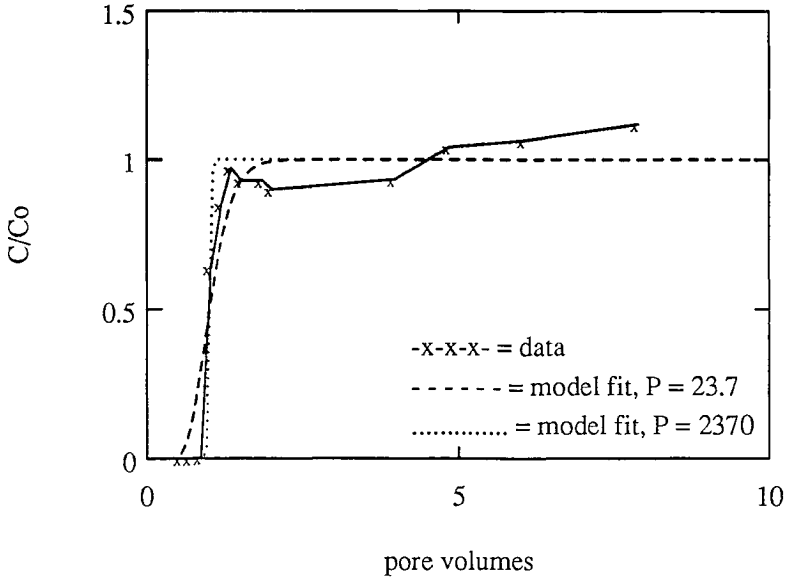

Figure 7: Trial-and-error model fits to the breakthrough curve of experiment 1: PRD1 break through at pH 7. Because of the apparent lack of sorption, the breakthrough curve is modeled in order to estimate the Peclet number. The one-site kinetic non-equilibrium model is used; R and β are equal to one, ω is equal to zero, and P is varied. A reasonable estimate of 237 for P is represented in the fitted curve in (a). Upper and lower bounds for P are shown in (b), where values of P are one order of magnitude higher and lower than in (a).

represents a choice for modeling purposes only and does not imply confidence of significance in all three digits.

For the conditions of experiments 1, 3 and 4, a P of 237 represents a coefficient of hydrodynamic dispersion (D) of 2.47×10^{-4} cm^2 s^{-1}. *Bales, et al. [1989]* obtained values of D ranging from 1.40×10^{-2} cm^2 s^{-1} to 1.73×10^{-2} cm^2 s^{-1} in soil-column experiments with bacteriophage MS-2 as the sorbent, a sandy soil as the sorbate, and flow rates averaging close to 10^{-2} cm s^{-1}. The smaller value of D for PRD1 in columns packed with sperical beads of small size range than for MS-2 in columns packed with a sandy soil may be reasonable due to the greater heterogeneity of natural soils. *Stocking [1989]* modeled breakthrough curves with a D of 1.08×10^{-4} cm^2 s^{-1} to 1.15×10^{-4} cm^2 s^{-1}; her experimental procedure was similar to that used in the PRD1 column experiments conducted in this research with the primary difference being the use of bacteriophage MS-2 instead of PRD1. Her values of D were taken to be equal to those of a conservative solute (NaCl) — not necessarily a valid assumption — but her model fits were reasonable. Her values for D are similar to the one used in this research. We shall later see that the value of P is only of minor importance in this set of experiments when we see that the breakthrough curves of experiments 3 and 4 are fairly insensitive to changes in P.

Experiments 3 and 4 were modeled with the two-site model in CFITIM [*Van Genuchten, 1981*]. Obtaining desorption rates was one of the primary motivations for this research, so our modeling efforts concentrated on determining a reasonable range of values for α, the desorption rate coefficient. In order to obtain such estimates, the adsorption curves and the desorption

curves of each of the two experiments were modeled with a variety of fixed and fitted parameters, always allowing the model to fit at least two of the parameters. Only the pH 5.5 portion of the desorption data was modeled; subsequent desorption steps would need to be modeled separately as they involved chemical perterbations. Adsorption and desorption curves were modeled separately because of poor performance of the model when given both curves to model as a unit. This poor performance may have been caused, in part, by the mass-balance problems previously mentioned. Because of anomalous results within the first pore volume of desorption, these data points were removed from the data set; these points were always unusually high, possibly caused by mechanical desorption resulting from jarring of the virus tubing during the changeover from virus-containing tubing to virus-free tubing when desorption was initiated.

From a family of curves produced for each adsorption and desorption curve, model fits bracketing the data and representing possible high and low estimates for α were selected. Figure 8 represents selected upper and lower bounds for the adsorption and desorption curves in experiment 3. The lower bound in figure 8a is concave down, with a small value of α; the upper bound in figure 8a is concave up, with a larger value of α. Desorption curves dropped off so slowly that curves produced by the model universally had nearly horizontal tails. Curves in figure 8b bound the pH 5.5 desorption limb of experiment 3.

Similar curves from the model for experiment 4 are presented in figure 9. Unlike the case of experiment 3, the model would not produce concave curves for the rising limb of experiment 4 but it produced instead curves that

(a) Bounding model curves for the adsorption limb of experiment 3.

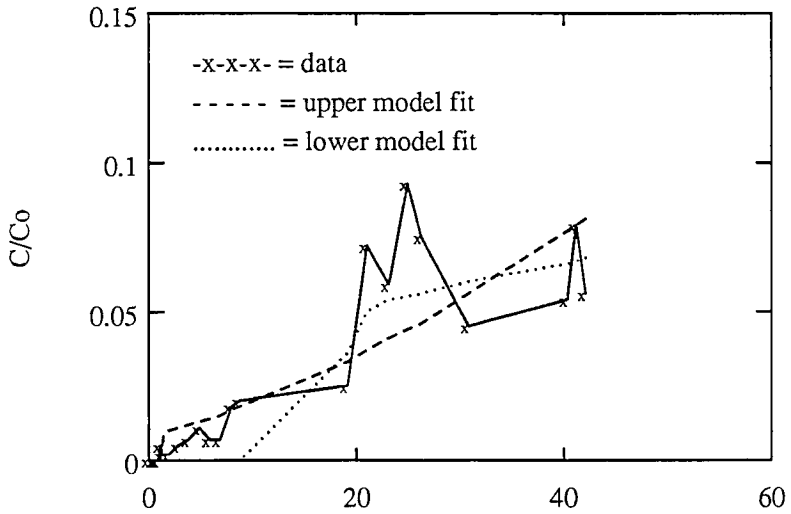

(b) Bounding model curves for the desorption limb of experiment 3.

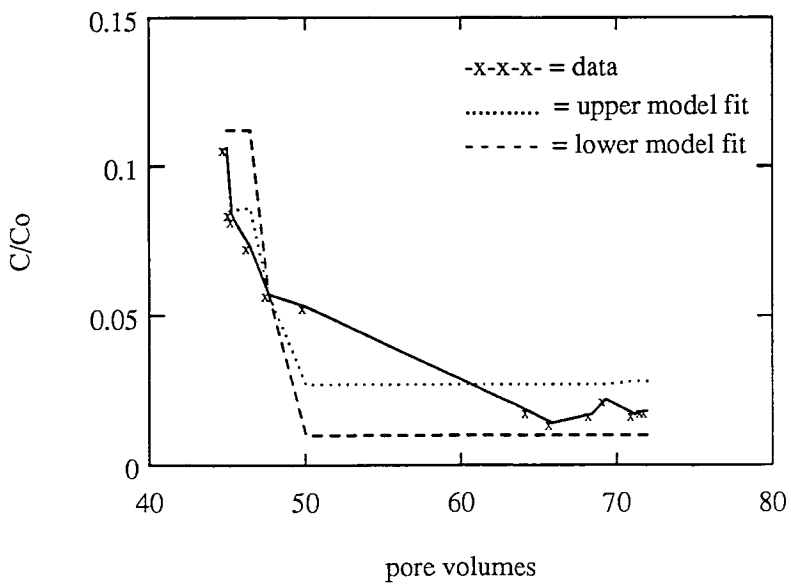

Figure 8: Model bracketing curves for column experiment 3. (a) shows bounding curves for the adsorption limb of the experiment; (b), the bounding curves for the pH 5.5 portion of the desorption limb. P is fixed at 237 in all model curves. The desorption rate coefficient (α) varies from 2.5×10^{-7} s^{-1} for the lower bounding curve in (b) to 6.7×10^{-6} s^{-1} for the upper bounding curve in (a). Other model parameters are listed in Table 1.

(a) Bounding model curves for the adsorption limb of experiment 4.

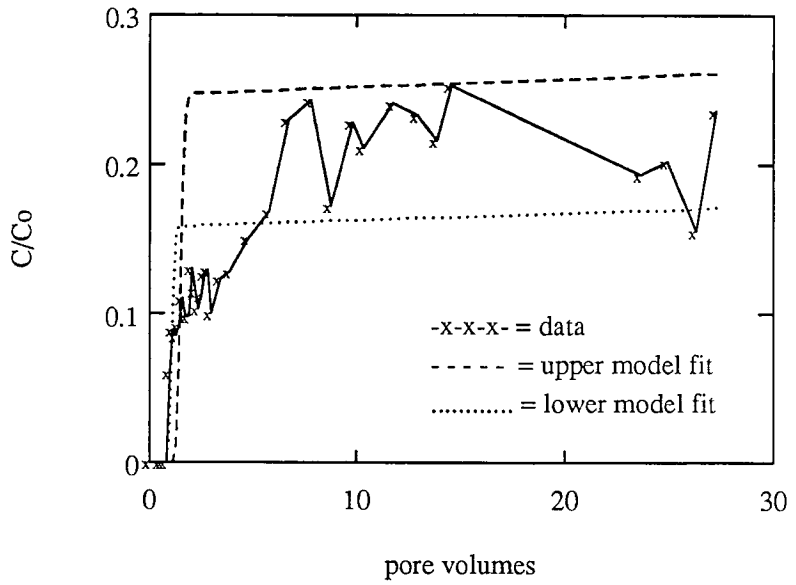

(b) Bounding model curves for the desorption limb of experiment 4.

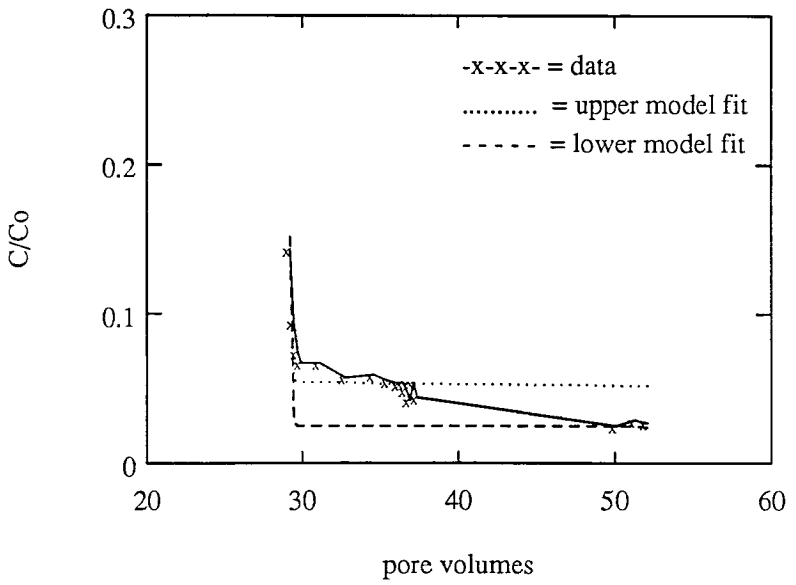

Figure 9: Model bracketing curves for column experiment 4. (a) shows bounding curves for the adsorption limb of the experiment; (b), the bounding curves for the pH 5.5 portion of the desorption limb. P is fixed at 237 in all model curves. The desorption rate coefficient (α) varies from 4.1×10^{-7} s^{-1} for the upper bounding curve in (a) to 1.5×10^{-6} s^{-1} for the upper bounding curve in (b). Other model parameters are listed in Table 1.

rose quickly and then leveled off with gently-rising slopes. Table 1 lists the fixed and fitted model parameters from this model bracketing excercise.

Values for α from these eight bounding curves ranged from 2.5×10^{-7} s^{-1} to 6.7×10^{-6} s^{-1} (0.022 day^{-1} to 0.58 day^{-1}). Given the scatter of the data and the non-unique nature of such curve-fitting, the true value of α may be considerably greater or less than this range. Although the variability of $\pm$ an order of magnitude or more is large, it can be seen that in our system steady-state desorption is negligible compared to the elution of phage resulting from perturbations in pH.

Stocking [*1989*] conducted similar column experiments but with bacteriophage MS-2 as the sorbent. Using the one-site kinetic non-equilibrium model, *Stocking* [*1989*] obtained values of α ranging from 4.1×10^{-5} s^{-1} to 2.8×10^{-4} s^{-1}. PRD1 appears to desorb much more slowly than MS-2.

Distribution coefficients obtained from modeling ranged from 41 cm^3 g^{-1} to 520 cm^3 g^{-1}. A comparison of adsorption and desorption rate coefficients showed that adsorption rates were 1.9×10^2 to 2.3×10^3 times as large as desorption rates.

Again comparing these results with those of *Stocking* [*1989*], a large difference in the model parameters between MS-2 and PRD1 becomes apparent. *Stocking* [*1989*] reports that the distribution coefficient for MS-2 to silica beads at pH 5 ranges from 0.37 to 0.69 cm^3 g^{-1}, two to three orders of magnitude smaller than the range for PRD-1 to identical beads. *Kroeger* [*1989*] reports a distribution coefficient of 41 cm^3 g^{-1} for MS-2 sorption to organosilane-modified silica (6.5% surface area coverage) at pH 5 and pH 7 in

Table 1. Model parameter values from the trial and error bracketing of the breakthrough curves of experiments 3 and 4[a].

fit[b]	R	SE[c]	K ($cm^3\ g^{-1}$)	β	SE[c]	F	ω	SE[c]	α ($10^{-6}\ s^{-1}$)	SSQ[d]
3a–	680	310	150	0.028	0.013	0.026	3.00*	-	1.2	0.0041
3a+	190	16	41	0.0068	0.0027	0.0015	4.80*	-	6.7	0.0064
3d–	2400	1600	520	0.0017	0.0011	0.0013	2.29*	-	0.25	0.0056
3d+	800*	-	180	0.0051	0.0003	0.0039	2.8	0.10	0.93	0.0020
4a–	1100	73	240	0.0010*	-	0.00010	1.9	0.060	0.44	0.082
4a+	890	2100	200	0.0017	0.0049	0.00058	1.40*	-	0.41	0.26
4d–	290	200	63	0.0038	0.35	0.00023	0.75*	-	0.68	0.017
4d+	250	21	54	0.0046	0.0004	0.00048	1.40*	-	1.5	0.0044

[a] The dimensionless model parameters P, R, β, and ω are defined in equations 9, 10, 12 and 13 respectively. The relationships between K and R, F and β, and α and ω are given in equations 10, 12 and 13, respectively. Parameter values marked with an asterisk (*) were fixed. Based upon the results of trial and error curve fitting to the conservative breakthrough curves of experiments 1 and 2, (figure 7), P was fixed at 237 in all model fits.

[b] 3 refers to experiment 3; 4, to experiment 4; a, to adsorption; d, to desorption; the minus sign, to the lower bound; the plus sign, to the upper bound.

[c] Standard error.

[d] Sum of square errors.

batch experiments. *Burge and Enkiri [1978]* report a distribution coefficient of 161 $cm^3\ g^{-1}$ for bacteriophage ΦX-174 sorption to a silt loam (f_{oc} of 0.0238) in batch experiments conducted at pH 6.2. The large distribution coefficient is probably due in part to the large surface area of the sample — 154 $m^2\ g^{-1}$. The estimated distribution coefficient for PRD1 is very large for bacteriophage sorption to an inorganic surface with a relatively small surface area. This suggests that sorption of PRD1, which is a lipid phage, may be largely driven by hydrophobic forces.

It is important to estimate the accuracy of these parameter values. Curve fitting with four unknown parameters leads to nonunique parameter values and hence to uncertainty. Furthermore, curve fitting to data with a large degree of variability increases the degree of uncertainty in the modeling. Bracketing the breakthrough curves represented an attempt to take the variability of the data into account. In an attempt to gain insight into the problem of nonuniqueness, an investigation into the sensitivity of the model fits to the parameters was undertaken. By varying the best-fit parameter values in a systematic way one at a time, the sensitivity of the model fits to changes in each of the parameters can be determined. Analysis was performed on both adsorption and desorption curves for the data of experiment 3, but only the adsorption plots are shown here as the desorption plots yielded similar information. Figure 10 illustrates the effects of varying P, β, R and ω, respectively, in the two-site kinetic sorption model.

In Figure 10a, the advection-dispersion equation is solved for values of P of 23.7 and 2370. It appears that varying P by an order of magnitude in either direction from the best-fit value of 237 produces negligible changes in

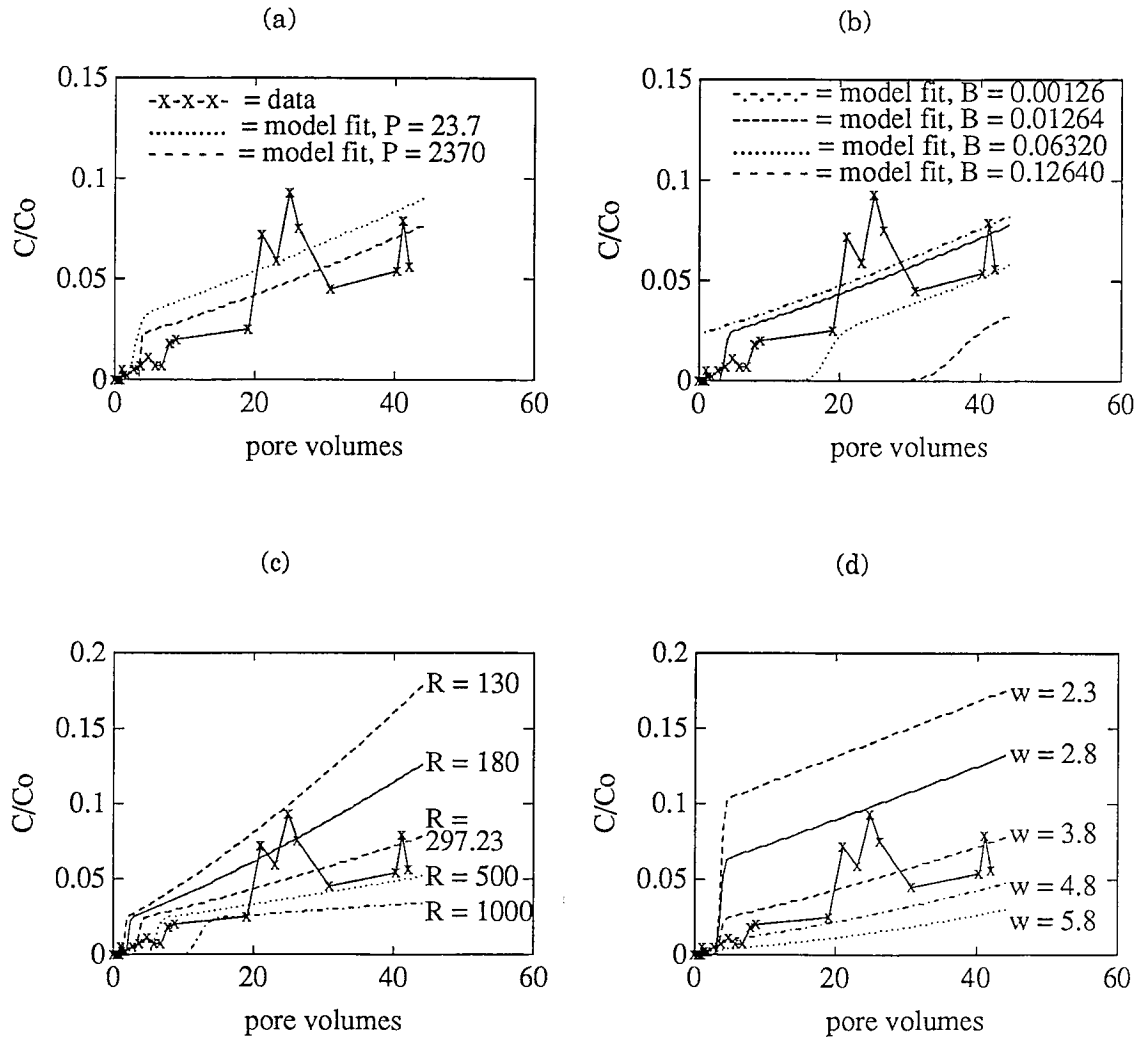

Figure 10. Graphs (a) through (d) represent various trial-and-error fits of the two-site kinetic non-eqilibrium model to the adsorption data of experiment 3. In (a) P was varied from 23.7 to 2370. The other parameters were fixed: R = 297.23, β = 0.01264, and ω = 3.80. It appears that when sorption is strong, as in the present case, the model is relatively insensitive to changes in P. In (b), β was varied from 0.00126 to 0.1264. The other parameters were fixed: P = 237; R and ω remained unchanged from (a). The model is sensitive to changes in β for large values of β and insensitive when β is small. In (c), R was varied from 130 to 1000. β = 0.01264; P and ω remained unchanged from (b). The model is sensitive to changes in R. In (d), ω is varied from 2.3 to 5.8. R = 297.23; P and β remained unchanged from (c). The model is sensitive to changes in ω.

the model fit. This implies that the model cannot accurately estimate values for P from experiments 3 and 4.

In Figure 10b, β is varied from its best-fit value of 0.01264; a range of values from 0.00126 to 0.12640 were tried. The model fit is relatively insensitive to reductions in β but is sensitive to increases in β. Thus β cannot be accurately estimated from these experiments.

β is small in all model fits, corresponding to a small value of F, the fraction of type 1 sites, but attempts to model the data with the 1-site model (in which β is equal to the inverse of R and hence drops out of the model) were unsuccessful, with model convergence upon unreasonable parameter values. The additional parameter in the two-site model is needed to describe the data. It may be that a multi-site model is needed to more accurately model virus sorption. Virus surfaces, like the surfaces of other biocolloids, are physically and chemically heterogeneous; more than two sorption mechanisms may be involved in virus sorption to immobile surfaces.

Figure 10c shows the sensitivity of the model to relatively small changes in R. The sensitivity of the model to changes in R suggests that the range of retardation factors obtained from the bracketing of the data, 190 to 2400, may represent an accurate range of values for R.

Figure 10d demonstrates the model sensitivity to ω. Small changes in ω result in significantly displaced curves, suggesting that the bounding values of ω for experiments 3 and 4, 0.75 to 4.8, may accurately bound the true value of ω.

CONCLUSIONS

Research was conducted in an attempt to quantitatively describe the sorption and transport of PRD1 in water-saturated silica columns. Breakthrough curves were modeled and transport parameters were estimated, providing order-of-magnitude insight into the contributions of pH and kinetics to virus sorption and transport.

pH can exert a major control on the sorption and transport of PRD1, and transient pH conditions appear to be effective in entraining sorbed phage. PRD1 sorbed to silica beads at pH 5.5 but did not sorb at pH 7.0. Most phage sorbed at pH 5.5 were eluted by raising solution pH by 1.5 to 2.5 pH units.

PRD1 sorption and transport in silica bead columns at a flow rate of 3.91×10^{-3} cm s^{-1} — a typical ground-water flow rate — are kinetically controlled. The distribution coefficient for PRD1 at pH 5.5 was estimated to fall in the range of 41 to 520 cm^3 g^{-1}; the ratio of the adsorption rate coefficient to the desorption rate coefficient, from 190 to 2400; and the desorption rate coefficient, 2.5×10^{-7} s^{-1} to 6.7×10^{-6} s^{-1}. The strong kinetic effect, evidenced in the slow rising limbs and the long tailing limbs of the breakthrough curves, is important because significant errors can result from the application of equilibrium sorption parameters to non-equilibrium situations. Furthermore, the small desorption rate coefficient is significant because of the effectiveness of high pH in entraining sorbed PRD1: an increase in system pH can have a greater impact upon virus transport than desorption occuring under steady-state conditions over long periods of time. On the other hand, an enterovirus with such a small desorption rate coefficient could, under steady-state

conditions, pose a significant *long-term* health risk to humans.

It is clear that many questions beg answers. In an effort to answer these questions, it would be highly desireable to improve elution techniques in order to achieve better mass balance. Among the important studies that are needed are column experiments in which the ionic strengths and divalent cation concentrations of the suspending solutions are varied in order to quantify the magnitude of the effects these variables have on sorption and transport of viruses. Column experiments with other oxide and organo-modified oxide surfaces are also needed.

APPENDIX

Results of column experiments

Experiment 1

64-minute pore volumes.

Seven stock samples, mean 1.05×10^5 pfu ml^{-1}.

Column packing: 15.27 g SiO_2, 0.0604 ± 0.0082 m^2 g^{-1}.

pore volume	C/C_o
Begin adsorption: pH 7.0, 0.02 M phosphate buffer with 0.08 M NaCl and 10^{-6} M calcium:	
0.54	0.000
0.70	0.000
0.86	0.003
1.02	0.63
1.19	0.85
1.35	0.97
1.51	0.93
1.84	0.93
2.00	0.90
3.97	0.93
4.86	1.04
6.07	1.06
7.89	1.12

Experiment 2

94-minute pore volumes.

Eleven stock samples, mean 0.915×10^5 pfu ml^{-1}.

Column packing: same column as experiment 1.

pore volume	C/C_o
Begin adsorption: pH 7.0, 0.02 M phosphate buffer with 0.08 M NaCl and 10^{-6} M calcium:	
0.00	0.001
0.66	0.001
0.83	0.004
1.00	0.42
1.15	0.90
1.32	0.92
1.49	1.02
1.65	0.88

1.81	0.96
1.98	0.97
2.14	1.07
2.31	1.00
2.48	0.96
2.92	1.12
3.96	1.06
4.93	0.98
5.94	1.04

Experiment 3

64-minute pore volumes.

Thirteen stock samples, mean 2.14×10^5 pfu ml^{-1}.

Column packing: 15.28 g SiO_2, 0.0604 ± 0.0082 m^2 g^{-1}.

Mass balance in 77.01 pore volumes of desorption: 82%.

pore volume	C/C_o

Begin adsorption: pH 5.5, 0.02 M phosphate buffer with 10^{-4} M calcium:

0.47	0.000
0.70	0.000
0.94	0.000
1.10	0.004
1.25	0.002
1.41	0.002
1.89	0.002
2.84	0.004
3.82	0.007
4.86	0.011
5.86	0.007
6.82	0.007
7.92	0.018
8.79	0.020
19.12	0.025
21.03	0.072
23.15	0.059
24.93	0.093
26.28	0.075
30.80	0.045
40.33	0.054
41.16	0.079
42.08	0.056

Begin desorption at pore volume 43.65: pH 5.5, phosphate buffer with 10^{-4} M calcium:

43.65	0.113
44.29	0.126

44.46	0.096
44.62	0.089
44.96	0.106
45.29	0.084
45.46	0.082
46.48	0.073
47.65	0.057
50.06	0.053
64.38	0.018
65.88	0.014
68.41	0.017
69.32	0.022

Begin desorption at pore volume 71.13: pH 7.0, calcium-free phosphate buffer:

71.13	0.017
71.69	0.018
71.94	0.018
72.18	13.85
72.43	14.27
72.68	8.23
72.93	5.38
73.18	3.95
73.43	3.64
73.67	2.95
73.92	2.50
74.81	1.78
75.83	1.95
76.79	1.75
78.29	0.59
88.19	0.31
91.33	0.18
95.15	0.15
113.91	0.12

Begin desorption at pore volume 115.40: pH 7.0, calcium-free phosphate buffer with 0.01 beef extract:

115.40	0.13
115.95	0.14
116.20	0.11
116.45	2.80
116.70	0.84
116.95	0.52
117.20	0.23
117.45	0.17
117.71	0.14
117.96	0.12
118.21	0.074
119.41	0.060
120.66	0.038

Experiment 4

64-minute pore volumes.

Ten stock samples, mean 3.89×10^5 pfu ml^{-1}.

Column packing: 15.26 g SiO_2, 0.0665 ± 0.0056 m^2 g^{-1}.

Mass balance in 135.36 pore volumes of desorption: 76%.

pore volume	C/C_o

Begin adsorption: pH 5.5, phosphate buffer with 10^{-6} M calcium, 64-minute pore volumes:

0	0.0000
0.53	0.0000
0.68	0.0000
0.83	0.0002
0.99	0.060
1.13	0.089
1.29	0.085
1.43	0.092
1.59	0.110
1.74	0.098
1.89	0.098
2.05	0.13
2.20	0.11
2.35	0.10
2.50	0.11
2.65	0.13
2.80	0.13
2.96	0.10
3.41	0.12
3.88	0.13
4.77	0.15
5.77	0.17
6.71	0.23
7.80	0.24
8.75	0.17
9.81	0.23
10.33	0.21
11.74	0.24
12.93	0.23
13.84	0.22
14.54	0.25
23.64	0.19
24.91	0.20
26.29	0.16
27.27	0.24

Begin desorption at pore volume 28.09: pH 5.5, phosphate buffer with 10^{-6} M calcium:

28.09	0.19

28.76	0.25
29.00	0.29
29.23	0.14
29.47	0.094
29.70	0.074
29.94	0.067
31.11	0.067
32.79	0.057
34.59	0.059

Begin desorption at pore volume 35.53: pH 5.5, calcium-free phosphate buffer:

35.53	0.055
36.19	0.053
36.43	0.054
36.67	0.049
36.91	0.042
37.14	0.054
37.38	0.044
50.08	0.025
51.29	0.029

Begin desorption at pore volume 52.09: pH 8.0, calcium-free phosphate buffer:

52.09	0.027
52.75	0.046
52.99	10.66
53.23	14.29
53.47	5.12
53.70	2.25
53.94	1.50
54.17	1.06
55.10	0.61
56.11	0.51
57.17	0.47
58.12	0.29
60.13	0.24
70.12	0.070
72.42	0.061
95.57	0.017
98.99	0.022
117.46	0.008
117.70	0.008

Begin desorption at pore volume 135.16: pH 8.0, calcium-free phosphate buffer with 0.025 beef extract and 0.01 Tween 80 detergent:

135.16	0.010
135.81	0.008
136.05	3.31
136.27	1.57
136.51	0.54
136.74	0.33
136.97	0.15

137.20	0.088
138.12	0.051
139.10	0.026
140.09	0.021

Begin desorption at pore volume 144.77: pH 9, calcium-free phosphate buffer with 0.025 beef extract and 0.01 Tween 80 detergent:

144.77	0.010
145.42	0.010
145.66	0.014
145.88	0.023
146.12	0.019
146.35	0.014
146.58	0.022
146.81	0.017
147.79	0.011
148.71	0.011
149.48	0.009
161.50	0.004
163.45	0.004

LITERATURE CITED

Bales, R. C., C. P. Gerba, G. H. Grondin, and S. L. Jensen, Bacteriophage transport in sandy soil and fractured tuff, *Applied and Environmental Microbiology*, *55*, 2061-2067, 1989.

Bear, J. and A. Verruijt, *Modeling Groundwater Flow and Pollution,* 414 pp., D. Reidel Publishing Company, Dordrecht , 1987.

Berg, G. R., B. Dean, and D. R. Dahling, Removal of poliovirus 1 from secondary effluents by lime flocculation and rapid sand filtration, *Journal of the American Water Works Association*, *60*, 193-198, 1968.

Burge, W. D. and N. K. Enkiri, Virus adsorption by five soils, *Journal of Environmental Quality*, *7*, 73-76, 1978.

Cameron, D. and A. Klute, Convective-Dispersive solute transport with combined equilibrium and kinetic adsorption model, *Water Resources Research*, *13*, 183-188, 1977.

Coates, K. and B. Smith, Dead end pore volume and dispersion in porous media, *Journal of the Society of Petroleum Engineers*, *4*, 73-84, 1964.

Craun, G. F., Waterborne disease — a status report emphasizing outbreaks in groundwater systems, *Groundwater*, *17*, 183-191, 1979.

Farrah, S., Chemical factors influencing adsorption of bacteriophage MS2 to membrane filters, *Applied and Environmental Microbiology*, *43*, 659-663, 1982.

Farrah, S., D. O. Shah, and L. O. Ingram , Effects of chaotropic and antichaotropic agents on elution of poliovirus adsorbed on membrane filters,

Proceedings of the National Academy of Science of the United States of America, *78*, 1229-1232, 1981.

Freeze, R. and J. Cherry, *Groundwater,* 604 pp., Prentice Hall, Inc., Englewood Cliffs, New Jersey, 1979.

Gerba, C. P., Applied and theoretical aspects of virus adsorption to surfaces, *Advances in Applied Microbiology*, *30*, 133-168, 1984.

Gschwend, P. M. and S. Wu, On the constancy of sediment-water partition coefficient of hydrophobic organic pollutants, *Environmental Science and Technology*, *19*, 90-96, 1985.

Ho, N. F. H. and W. I. Higuchi, Preferential aggregation and coalescence in heterodispersed systems, *Journal of Pharmaceutical Sciences*, *57*, 436-442, 1968.

Hurst, C. J., C. P. Gerba, and I. Cech, Effects of environmental variables and soil characteristics on virus survival in soil, *Applied and Environmental Microbiology*, *40*, 1067-1079, 1980.

Iler, R. K., *The Chemistry of Silica,* 637 pp., Wiley, New York, 1979.

Kauzmann, W., Some factors in the interpretation of protein denaturation, *Advances in Protein Chemistry*, *14*, 1-63, 1959.

Kroeger, T. W., Hydrophobic Partitioning of the Bacteriophage MS-2, M.S. Thesis, 104 pp., Department of Hydrology and Water Resources, University of Arizona, Tucson, AZ, 1989.

Mix, T. W., The physical chemistry of membrane-virus interaction, *Developments in Industrial Microbiology*, *15*, 136-142, 1974.

Murray, J. P. and G. A. Parks, Poliovirus adsorption on oxide surfaces: correspondence with the DLVO-Lifshitz theory of colloid stability, in *Particulates in Water*, edited by M. C. Kavanaugh and J. O. Leckie , Advances in Chemistry Series 189, pp. 97-133, American Chemical Society, Washington, D.C. , 1980.

O'Conner, D. J. and J. P. Connolly, The effect of concentration of adsorbing solids on the partition coefficient, *Water Research*, *14*, 1517-1523, 1980.

Olsen, R. H., J. Siak, and R. Gray, Characteristics of PRD1, a plasmid-dependent broad host range DNA Bacteriophage , *Journal of Virology*, *14*, 689-699, 1974.

Popovic, M. and W. D. Deckwer, Transient behavior of reactors with dispersion and stagnant zones, *Chemical Engineering Journal*, *11*, 67-72, 1976.

Rajagopalan, R. and J. S. Kim, Adsorption of brownian particles in the presence of potential barriers: effect of different modes of double-layer interaction, *Journal of Colloid and Interface Science*, *83*, 428-448, 1981.

Reddy, K. R., R. Khaleel, and M. R. Overcash, Behavior and transport of microbial pathogens and indicator organisms in soils treated with organic wastes, *Journal of Environmental Quality*, *10*, 255-266, 1981.

Schenkel, J. H. and J. A. Kitchener, A test of the Derjaguin-Verwey-Overbeek theory with a colloidal suspension, *Transactions of the Faraday Society*, *56*, 161-173, 1960.

Snyder, L. R. and J. J. Kirkland, *Introduction to Modern Liquid Chromatography, 2nd ed.,* 863 pp., Wiley, New York, 1979.

Stocking, K., Adsorption of MS-2 Bacteriophage to Silica, M.S. Thesis, 91 pp., Department of Hydrology and Water Resources, University of Arizona, Tucson, AZ, 1989.

Stumm, W. and J. J. Morgan, *Aquatic Chemistry,* 780 pp., Wiley, New York, 1981.

VanGenuchten, M. Th., Non-equilibrium transport parameters from miscible displacement experiments, *Research Report 119*, 88 pp., U. S. Salinity Lab, Riverside, CA, 1981.

VanGenuchten, M. Th. and P. J. Wierenga, Numerical solution for convective dispersion with intra-aggregate diffusion and non-linear adsorption, in *System Simulation in Water Resources*, edited by C. G. Vansteenkiste, pp. 275-291, North-Holland , Amsterdam, 1976.

Verwey, E. J. W. and J. T. G. Overbeek, *Theory of the Stability of Lyophobic Colloids,* 205 pp., Elsevier, New York, 1948.

Vinten, A. J. A., B. Yaron, and P. H. Nye, Vertical transport of pesticides into soil when adsorbed on suspended particles, *Journal of Agricultural and Food Chemistry*, *31*, 662-664, 1983.

Wallis, C. and J. L. Melnick, Concentration of enteroviruses on membrane filters, *Journal of Virology*, *1*, 472-477, 1967.

Westwood, J. C. N. and S. A. Sattar, The minimal infective dose, in *Viruses in Water*, edited by G. Berg, H. L. Bodily, E. H. Lennette, J. L. Melnick and T. G. Metcalf, pp. 61-69, American Public Health Association, Washington, D.C., 1976.

Yates, M. V., C. P. Gerba, and L. M. Kelley, Virus persistence in groundwater, *Applied and Environmental Microbiology*, *49*, 778-781, 1985.

Yates, M. V., S. R. Yates, J. Wagner, and C. P. Gerba, Modeling virus survival and transport in the subsurface, *Journal of Contaminant Hydrology*, *1*, 329-345, 1987.